

Measurement of the $t\bar{t}$ production cross section with an *in situ* calibration of b -jet identification efficiency

T. Aaltonen,²² B. Álvarez González,^{10,w} S. Amerio,^{42a} D. Amidei,³³ A. Anastassov,³⁷ A. Annovi,¹⁸ J. Antos,¹³ G. Apollinari,¹⁶ J. A. Appel,¹⁶ A. Apresyan,⁴⁷ T. Arisawa,⁵⁶ A. Artikov,¹⁴ J. Asaadi,⁵² W. Ashmanskas,¹⁶ B. Auerbach,⁵⁹ A. Aurisano,⁵² F. Azfar,⁴¹ W. Badgett,¹⁶ A. Barbaro-Galtieri,²⁷ V. E. Barnes,⁴⁷ B. A. Barnett,²⁴ P. Barria,^{45c,45a} P. Bartos,¹³ M. Baucus,^{42b,42a} G. Bauer,³¹ F. Bedeschi,^{45a} D. Beecher,²⁹ S. Behari,²⁴ G. Bellettini,^{45b,45a} J. Bellinger,⁵⁸ D. Benjamin,¹⁵ A. Beretvas,¹⁶ A. Bhatti,⁴⁹ M. Binkley,^{16,a} D. Bisello,^{42b,42a} I. Bizjak,^{29,cc} K. R. Bland,⁵ C. Blocker,⁷ B. Blumenfeld,²⁴ A. Bocci,¹⁵ A. Bodek,⁴⁸ D. Bortoletto,⁴⁷ J. Boudreau,⁴⁶ A. Boveia,¹² B. Brau,^{16,b} L. Brigliadori,^{6b,6a} A. Brisuda,¹³ C. Bromberg,³⁴ E. Brucken,²² M. Bucciantonio,^{45b,45a} J. Budagov,¹⁴ H. S. Budd,⁴⁸ S. Budd,²³ K. Burkett,¹⁶ G. Busetto,^{42b,42a} P. Bussey,²⁰ A. Buzatu,³² S. Cabrera,^{15,y} C. Calancha,³⁰ S. Camarda,⁶⁰ M. Campanelli,³⁴ M. Campbell,³³ F. Canelli,^{12,16} A. Canepa,⁴⁴ B. Carls,²³ D. Carlsmith,⁵⁸ R. Carosi,^{45a} S. Carrillo,^{17,1} S. Carron,¹⁶ B. Casal,¹⁰ M. Casarsa,¹⁶ A. Castro,^{6b,6a} P. Catastini,¹⁶ D. Cauz,^{53a} V. Cavaliere,^{45a} M. Cavalli-Sforza,⁶⁰ A. Cerri,^{27,g} L. Cerrito,^{29,r} Y. C. Chen,¹ M. Chertok,⁸ G. Chiarelli,^{45a} G. Chlachidze,¹⁶ F. Chlebana,¹⁶ K. Cho,²⁶ D. Chokheli,¹⁴ J. P. Chou,²¹ W. H. Chung,⁵⁸ Y. S. Chung,⁴⁸ C. I. Ciobanu,⁴³ M. A. Ciocci,^{45c,45a} A. Clark,¹⁹ D. Clark,⁷ G. Compostella,^{42b,42a} M. E. Convery,¹⁶ J. Conway,⁸ M. Corbo,⁴³ M. Cordelli,¹⁸ C. A. Cox,⁸ D. J. Cox,⁸ F. Crescioli,^{45b,45a} C. Cuenca Almenar,⁵⁹ J. Cuevas,^{10,w} R. Culbertson,¹⁶ D. Dagenhart,¹⁶ N. d'Ascenzo,^{43,u} M. Datta,¹⁶ P. de Barbaro,⁴⁸ S. De Cecco,^{50a} G. De Lorenzo,⁶⁰ M. Dell'Orso,^{45b,45a} C. Deluca,⁶⁰ L. Demortier,⁴⁹ J. Deng,^{15,d} M. Deninno,^{6a} F. Devoto,²² M. d'Errico,^{42b,42a} A. Di Canto,^{45b,45a} B. Di Ruzza,^{45a} J. R. Dittmann,⁵ M. D'Onofrio,²⁸ S. Donati,^{45b,45a} P. Dong,¹⁶ T. Dorigo,^{42a} K. Ebina,⁵⁶ A. Elagin,⁵² A. Eppig,³³ R. Erbacher,⁸ D. Errede,²³ S. Errede,²³ N. Ershaidat,^{43,bb} R. Eusebi,⁵² H. C. Fang,²⁷ S. Farrington,⁴¹ M. Feindt,²⁵ J. P. Fernandez,³⁰ C. Ferrazza,^{45d,45a} R. Field,¹⁷ G. Flanagan,^{47,s} R. Forrest,⁸ M. J. Frank,⁵ M. Franklin,²¹ J. C. Freeman,¹⁶ I. Furic,¹⁷ M. Gallinaro,⁴⁹ J. Galyardt,¹¹ J. E. Garcia,¹⁹ A. F. Garfinkel,⁴⁷ P. Garosi,^{45c,45a} H. Gerberich,²³ E. Gerchtein,¹⁶ S. Giagu,^{50b,50a} V. Giakoumopoulou,³ P. Giannetti,^{45a} K. Gibson,⁴⁶ C. M. Ginsburg,¹⁶ N. Giokaris,³ P. Giromini,¹⁸ M. Giunta,^{45a} G. Giurgiu,²⁴ V. Glagolev,¹⁴ D. Glenzinski,¹⁶ M. Gold,³⁶ D. Goldin,⁵² N. Goldschmidt,¹⁷ A. Golossanov,¹⁶ G. Gomez,¹⁰ G. Gomez-Ceballos,³¹ M. Goncharov,³¹ O. González,³⁰ I. Gorelov,³⁶ A. T. Goshaw,¹⁵ K. Goulianos,⁴⁹ A. Gresele,^{42a} S. Grinstein,⁶⁰ C. Grosso-Pilcher,¹² R. C. Group,¹⁶ J. Guimaraes da Costa,²¹ Z. Gunay-Unalan,³⁴ C. Haber,²⁷ S. R. Hahn,¹⁶ E. Halkiadakis,⁵¹ A. Hamaguchi,⁴⁰ J. Y. Han,⁴⁸ F. Happacher,¹⁸ K. Hara,⁵⁴ D. Hare,⁵¹ M. Hare,⁵⁵ R. F. Harr,⁵⁷ K. Hatakeyama,⁵ C. Hays,⁴¹ M. Heck,²⁵ J. Heinrich,⁴⁴ M. Herndon,⁵⁸ S. Hewamanage,⁵ D. Hidas,⁵¹ A. Hocker,¹⁶ W. Hopkins,^{16,h} D. Horn,²⁵ S. Hou,¹ R. E. Hughes,³⁸ M. Hurwitz,¹² U. Husemann,⁵⁹ N. Hussain,³² M. Hussein,³⁴ J. Huston,³⁴ G. Introzzi,^{45a} M. Iori,^{50b,50a} A. Ivanov,^{8,p} E. James,¹⁶ D. Jang,¹¹ B. Jayatilaka,¹⁵ E. J. Jeon,²⁶ M. K. Jha,^{6a} S. Jindariani,¹⁶ W. Johnson,⁸ M. Jones,⁴⁷ K. K. Joo,²⁶ S. Y. Jun,¹¹ T. R. Junk,¹⁶ T. Kamon,⁵² P. E. Karchin,⁵⁷ Y. Kato,^{40,o} W. Ketchum,¹² J. Keung,⁴⁴ V. Khotilovich,⁵² B. Kilminster,¹⁶ D. H. Kim,²⁶ H. S. Kim,²⁶ H. W. Kim,²⁶ J. E. Kim,²⁶ M. J. Kim,¹⁸ S. B. Kim,²⁶ S. H. Kim,⁵⁴ Y. K. Kim,¹² N. Kimura,⁵⁶ S. Klimenko,¹⁷ K. Kondo,⁵⁶ D. J. Kong,²⁶ J. Konigsberg,¹⁷ A. Korytov,¹⁷ A. V. Kotwal,¹⁵ M. Kreps,²⁵ J. Kroll,⁴⁴ D. Krop,¹² N. Krumnack,^{5,m} M. Kruse,¹⁵ V. Krutelyov,^{52,e} T. Kuhr,²⁵ M. Kurata,⁵⁴ S. Kwang,¹² A. T. Laasanen,⁴⁷ S. Lami,^{45a} S. Lammel,¹⁶ M. Lancaster,²⁹ R. L. Lander,⁸ K. Lannon,^{38,v} A. Lath,⁵¹ G. Latino,^{45c,45a} I. Lazzizzera,^{42a} T. LeCompte,² E. Lee,⁵² H. S. Lee,¹² J. S. Lee,²⁶ S. W. Lee,^{52,x} S. Leo,^{45b,45a} S. Leone,^{45a} J. D. Lewis,¹⁶ C.-J. Lin,²⁷ J. Linacre,⁴¹ M. Lindgren,¹⁶ E. Lipeles,⁴⁴ A. Lister,¹⁹ D. O. Litvintsev,¹⁶ C. Liu,⁴⁶ Q. Liu,⁴⁷ T. Liu,¹⁶ S. Lockwitz,⁵⁹ N. S. Lockyer,⁴⁴ A. Loginov,⁵⁹ D. Lucchesi,^{42b,42a} J. Lueck,²⁵ P. Lujan,²⁷ P. Lukens,¹⁶ G. Lungu,⁴⁹ J. Lys,²⁷ R. Lysak,¹³ R. Madrak,¹⁶ K. Maeshima,¹⁶ K. Makhoul,³¹ P. Maksimovic,²⁴ S. Malik,⁴⁹ G. Manca,^{28,c} A. Manousakis-Katsikakis,³ F. Margaroli,⁴⁷ C. Marino,²⁵ M. Martínez,⁶⁰ R. Martínez-Ballarín,³⁰ P. Mastrandrea,^{50a} M. Mathis,²⁴ M. E. Mattson,⁵⁷ P. Mazzanti,^{6a} K. S. McFarland,⁴⁸ P. McIntyre,⁵² R. McNulty,^{28,j} A. Mehta,²⁸ P. Mehtala,²² A. Menzione,^{45a} C. Mesropian,⁴⁹ T. Miao,¹⁶ D. Mietlicki,³³ A. Mitra,¹ G. Mitselmakher,¹⁷ H. Miyake,⁵⁴ S. Moed,²¹ N. Moggi,^{6a} M. N. Mondragon,^{16,1} C. S. Moon,²⁶ R. Moore,¹⁶ M. J. Morello,¹⁶ J. Morlock,²⁵ P. Movilla Fernandez,¹⁶ A. Mukherjee,¹⁶ Th. Muller,²⁵ P. Murat,¹⁶ M. Mussini,^{6b,6a} J. Nachtman,^{16,n} Y. Nagai,⁵⁴ J. Naganoma,⁵⁶ I. Nakano,³⁹ A. Napier,⁵⁵ J. Nett,⁵⁸ C. Neu,^{44,aa} M. S. Neubauer,²³ J. Nielsen,^{27,f} L. Nodulman,² O. Normiella,²³ E. Nurse,²⁹ L. Oakes,⁴¹ S. H. Oh,¹⁵ Y. D. Oh,²⁶ I. Oksuzian,¹⁷ T. Okusawa,⁴⁰ R. Orava,²² L. Ortolan,⁶⁰ S. Pagan Griso,^{42b,42a} C. Pagliarone,^{53a} E. Palencia,^{10,g} V. Papadimitriou,¹⁶ A. A. Paramonov,² J. Patrick,¹⁶ G. Pauletta,^{53b,53a} M. Paulini,¹¹ C. Paus,³¹ D. E. Pellett,⁸ A. Penzo,^{53a} T. J. Phillips,¹⁵ G. Piacentino,^{45a} E. Pianori,⁴⁴ J. Pilot,³⁸ K. Pitts,²³ C. Plager,⁹ L. Pondrom,⁵⁸ K. Potamianos,⁴⁷ O. Poukhov,^{14,a} F. Prokoshin,^{14,z} A. Pronko,¹⁶ F. Ptohos,^{18,i} E. Pueschel,¹¹ G. Punzi,^{45b,45a} J. Pursley,⁵⁸ A. Rahaman,⁴⁶ V. Ramakrishnan,⁵⁸ N. Ranjan,⁴⁷ I. Redondo,³⁰ P. Renton,⁴¹ M. Rescigno,^{50a} F. Rimondi,^{6b,6a}

L. Ristori,^{45a,16} A. Robson,²⁰ T. Rodrigo,¹⁰ T. Rodriguez,⁴⁴ E. Rogers,²³ S. Rolli,⁵⁵ R. Roser,¹⁶ M. Rossi,^{53a}
 F. Ruffini,^{45c,45a} A. Ruiz,¹⁰ J. Russ,¹¹ V. Rusu,¹⁶ A. Safonov,⁵² W. K. Sakumoto,⁴⁸ L. Santi,^{53b,53a} L. Sartori,^{45a} K. Sato,⁵⁴
 V. Saveliev,^{43,u} A. Savoy-Navarro,⁴³ P. Schlabach,¹⁶ A. Schmidt,²⁵ E. E. Schmidt,¹⁶ M. P. Schmidt,^{59,a} M. Schmitt,³⁷
 T. Schwarz,⁸ L. Scodellaro,¹⁰ A. Scribano,^{45c,45a} F. Scuri,^{45a} A. Sedov,⁴⁷ S. Seidel,³⁶ Y. Seiya,⁴⁰ A. Semenov,¹⁴
 F. Sforza,^{45b,45a} A. Sfyrta,²³ S. Z. Shalhout,⁸ T. Shears,²⁸ P. F. Shepard,⁴⁶ M. Shimojima,^{54,t} S. Shiraishi,¹² M. Shochet,¹²
 I. Shreyber,³⁵ A. Simonenko,¹⁴ P. Sinervo,³² A. Sissakian,^{14,a} K. Sliwa,⁵⁵ J. R. Smith,⁸ F. D. Snider,¹⁶ A. Soha,¹⁶
 S. Somalwar,⁵¹ V. Sorin,⁶⁰ P. Squillacioti,¹⁶ M. Stanitzki,⁵⁹ R. St. Denis,²⁰ B. Stelzer,³² O. Stelzer-Chilton,³² D. Stentz,³⁷
 J. Strologas,³⁶ G. L. Strycker,³³ Y. Sudo,⁵⁴ A. Sukhanov,¹⁷ I. Suslov,¹⁴ K. Takemasa,⁵⁴ Y. Takeuchi,⁵⁴ J. Tang,¹²
 M. Tecchio,³³ P. K. Teng,¹ J. Thom,^{16,h} J. Thome,¹¹ G. A. Thompson,²³ E. Thomson,⁴⁴ P. Tito-Guzmán,³⁰ S. Tkaczyk,¹⁶
 D. Toback,⁵² S. Tokar,¹³ K. Tollefson,³⁴ T. Tomura,⁵⁴ D. Tonelli,¹⁶ S. Torre,¹⁸ D. Torretta,¹⁶ P. Totaro,^{53b,53a}
 M. Trovato,^{45d,45a} Y. Tu,⁴⁴ N. Turini,^{45c,45a} F. Ukegawa,⁵⁴ S. Uozumi,²⁶ A. Varganov,³³ E. Vataga,^{45d,45a} F. Vázquez,^{17,1}
 G. Velev,¹⁶ C. Vellidis,³ M. Vidal,³⁰ I. Vila,¹⁰ R. Vilar,¹⁰ M. Vogel,³⁶ G. Volpi,^{45b,45a} P. Wagner,⁴⁴ R. L. Wagner,¹⁶
 T. Wakisaka,⁴⁰ R. Wallny,⁹ S. M. Wang,¹ A. Warburton,³² D. Waters,²⁹ M. Weinberger,⁵² W. C. Wester III,¹⁶
 B. Whitehouse,⁵⁵ D. Whiteson,^{44,d} A. B. Wicklund,² E. Wicklund,¹⁶ S. Wilbur,¹² F. Wick,²⁵ H. H. Williams,⁴⁴
 J. S. Wilson,³⁸ P. Wilson,¹⁶ B. L. Winer,³⁸ P. Wittich,^{16,h} S. Wolbers,¹⁶ H. Wolfe,³⁸ T. Wright,³³ X. Wu,¹⁹ Z. Wu,⁵
 K. Yamamoto,⁴⁰ J. Yamaoka,¹⁵ U. K. Yang,^{12,q} Y. C. Yang,²⁶ W.-M. Yao,²⁷ G. P. Yeh,¹⁶ K. Yi,^{16,n} J. Yoh,¹⁶ K. Yorita,⁵⁶
 T. Yoshida,^{40,k} G. B. Yu,¹⁵ I. Yu,²⁶ S. S. Yu,¹⁶ J. C. Yun,¹⁶ A. Zanetti,^{53a} Y. Zeng,¹⁵ and S. Zucchelli^{6b,6a}

(CDF Collaboration)

¹*Institute of Physics, Academia Sinica, Taipei, Taiwan 11529, Republic of China*²*Argonne National Laboratory, Argonne, Illinois 60439, USA*³*University of Athens, 157 71 Athens, Greece*⁴*Institut de Física d'Altes Energies, ICREA, Universitat Autònoma de Barcelona, E-08193, Bellaterra (Barcelona), Spain*⁵*Baylor University, Waco, Texas 76798, USA*^{6a}*Istituto Nazionale di Fisica Nucleare Bologna, I-40127 Bologna, Italy*^{6b}*University of Bologna, I-40127 Bologna, Italy*⁷*Brandeis University, Waltham, Massachusetts 02254, USA*⁸*University of California, Davis, Davis, California 95616, USA*⁹*University of California, Los Angeles, Los Angeles, California 90024, USA*¹⁰*Instituto de Física de Cantabria, CSIC-University of Cantabria, 39005 Santander, Spain*¹¹*Carnegie Mellon University, Pittsburgh, Pennsylvania 15213, USA*¹²*Enrico Fermi Institute, University of Chicago, Chicago, Illinois 60637, USA*¹³*Comenius University, 842 48 Bratislava, Slovakia; Institute of Experimental Physics, 040 01 Kosice, Slovakia*¹⁴*Joint Institute for Nuclear Research, RU-141980 Dubna, Russia*¹⁵*Duke University, Durham, North Carolina 27708, USA*¹⁶*Fermi National Accelerator Laboratory, Batavia, Illinois 60510, USA*¹⁷*University of Florida, Gainesville, Florida 32611, USA*¹⁸*Laboratori Nazionali di Frascati, Istituto Nazionale di Fisica Nucleare, I-00044 Frascati, Italy*¹⁹*University of Geneva, CH-1211 Geneva 4, Switzerland*²⁰*Glasgow University, Glasgow G12 8QQ, United Kingdom*²¹*Harvard University, Cambridge, Massachusetts 02138, USA*²²*Division of High Energy Physics, Department of Physics,**University of Helsinki and Helsinki Institute of Physics, FIN-00014, Helsinki, Finland*²³*University of Illinois, Urbana, Illinois 61801, USA*²⁴*The Johns Hopkins University, Baltimore, Maryland 21218, USA*²⁵*Institut für Experimentelle Kernphysik, Karlsruhe Institute of Technology, D-76131 Karlsruhe, Germany*²⁶*Center for High Energy Physics: Kyungpook National University, Daegu 702-701, Korea;**Seoul National University, Seoul 151-742, Korea; Sungkyunkwan University, Suwon 440-746, Korea;**Korea Institute of Science and Technology Information, Daejeon 305-806, Korea; Chonnam National University,**Gwangju 500-757, Korea; Chonbuk National University, Jeonju 561-756, Korea*²⁷*Ernest Orlando Lawrence Berkeley National Laboratory, Berkeley, California 94720, USA*²⁸*University of Liverpool, Liverpool L69 7ZE, United Kingdom*²⁹*University College London, London WC1E 6BT, United Kingdom*³⁰*Centro de Investigaciones Energéticas Medioambientales y Tecnológicas, E-28040 Madrid, Spain*³¹*Massachusetts Institute of Technology, Cambridge, Massachusetts 02139, USA*

- ³²*Institute of Particle Physics: McGill University, Montréal, Québec, Canada H3A 2T8; Simon Fraser University, Burnaby, British Columbia, Canada V5A 1S6; University of Toronto, Toronto, Ontario, Canada M5S 1A7; and TRIUMF, Vancouver, British Columbia, Canada V6T 2A3*
- ³³*University of Michigan, Ann Arbor, Michigan 48109, USA*
- ³⁴*Michigan State University, East Lansing, Michigan 48824, USA*
- ³⁵*Institution for Theoretical and Experimental Physics, ITEP, Moscow 117259, Russia*
- ³⁶*University of New Mexico, Albuquerque, New Mexico 87131, USA*
- ³⁷*Northwestern University, Evanston, Illinois 60208, USA*
- ³⁸*The Ohio State University, Columbus, Ohio 43210, USA*
- ³⁹*Okayama University, Okayama 700-8530, Japan*
- ⁴⁰*Osaka City University, Osaka 588, Japan*
- ⁴¹*University of Oxford, Oxford OX1 3RH, United Kingdom*
- ^{42a}*Istituto Nazionale di Fisica Nucleare, Sezione di Padova-Trento, I-35131 Padova, Italy*
- ^{42b}*University of Padova, I-35131 Padova, Italy*
- ⁴³*LPNHE, Université Pierre et Marie Curie/IN2P3-CNRS, UMR7585, Paris, F-75252 France*
- ⁴⁴*University of Pennsylvania, Philadelphia, Pennsylvania 19104, USA*
- ^{45a}*Istituto Nazionale di Fisica Nucleare Pisa, I-56127 Pisa, Italy*
- ^{45b}*University of Pisa, I-56127 Pisa, Italy*
- ^{45c}*University of Siena, I-56127 Pisa, Italy*
- ^{45d}*Scuola Normale Superiore, I-56127 Pisa, Italy*
- ⁴⁶*University of Pittsburgh, Pittsburgh, Pennsylvania 15260, USA*
- ⁴⁷*Purdue University, West Lafayette, Indiana 47907, USA*
- ⁴⁸*University of Rochester, Rochester, New York 14627, USA*
- ⁴⁹*The Rockefeller University, New York, New York 10065, USA*
- ^{50a}*Istituto Nazionale di Fisica Nucleare, Sezione di Roma 1, I-00185 Roma, Italy*
- ^{50b}*Sapienza Università di Roma, I-00185 Roma, Italy*
- ⁵¹*Rutgers University, Piscataway, New Jersey 08855, USA*

^aDeceased.

^bVisitor from University of Massachusetts Amherst, Amherst, Massachusetts 01003.

^cVisitor from Istituto Nazionale di Fisica Nucleare, Sezione di Cagliari, 09042 Monserrato (Cagliari), Italy.

^dVisitor from University of California Irvine, Irvine, CA 92697.

^eVisitor from University of California Santa Barbara, Santa Barbara, CA 93106.

^fVisitor from University of California Santa Cruz, Santa Cruz, CA 95064.

^gVisitor from CERN, CH-1211 Geneva, Switzerland.

^hVisitor from Cornell University, Ithaca, NY 14853.

ⁱVisitor from University of Cyprus, Nicosia CY-1678, Cyprus.

^jVisitor from University College Dublin, Dublin 4, Ireland.

^kVisitor from University of Fukui, Fukui City, Fukui Prefecture, Japan 910-0017.

^lVisitor from Universidad Iberoamericana, Mexico D.F., Mexico.

^mVisitor from Iowa State University, Ames, IA 50011.

ⁿVisitor from University of Iowa, Iowa City, IA 52242.

^oVisitor from Kinki University, Higashi-Osaka City, Japan 577-8502.

^pVisitor from Kansas State University, Manhattan, KS 66506.

^qVisitor from University of Manchester, Manchester M13 9PL, England.

^rVisitor from Queen Mary, University of London, London, E1 4NS, England.

^sVisitor from Muons, Inc., Batavia, IL 60510.

^tVisitor from Nagasaki Institute of Applied Science, Nagasaki, Japan.

^uVisitor from National Research Nuclear University, Moscow, Russia.

^vVisitor from University of Notre Dame, Notre Dame, IN 46556.

^wVisitor from Universidad de Oviedo, E-33007 Oviedo, Spain.

^xVisitor from Texas Tech University, Lubbock, TX 79609.

^yVisitor from IFIC(CSIC-Universitat de Valencia), 56071 Valencia, Spain.

^zVisitor from Universidad Técnica Federico Santa María, 110v Valparaíso, Chile.

^{aa}Visitor from University of Virginia, Charlottesville, VA 22906.

^{bb}Visitor from Yarmouk University, Irbid 211-63, Jordan.

^{cc}On leave from J. Stefan Institute, Ljubljana, Slovenia.

⁵²*Texas A University, College Station, Texas 77843, USA*^{53a}*Istituto Nazionale di Fisica Nucleare Trieste/Udine, I-34100 Trieste, I-33100 Udine, Italy*^{53b}*University of Trieste/Udine, I-33100 Udine, Italy*⁵⁴*University of Tsukuba, Tsukuba, Ibaraki 305, Japan*⁵⁵*Tufts University, Medford, Massachusetts 02155, USA*⁵⁶*Waseda University, Tokyo 169, Japan*⁵⁷*Wayne State University, Detroit, Michigan 48201, USA*⁵⁸*University of Wisconsin, Madison, Wisconsin 53706, USA*⁵⁹*Yale University, New Haven, Connecticut 06520, USA*⁶⁰*Institut de Fisica d'Altes Energies, ICREA, Universitat Autònoma de Barcelona, E-08193, Bellaterra (Barcelona), Spain*

(Received 14 October 2010; published 13 April 2011)

A measurement of the top-quark pair-production cross section in $p\bar{p}$ collisions at $\sqrt{s} = 1.96$ TeV using data corresponding to an integrated luminosity of 1.12 fb^{-1} collected with the Collider Detector at Fermilab is presented. Decays of top-quark pairs into the final states $e\nu + \text{jets}$ and $\mu\nu + \text{jets}$ are selected, and the cross section and the b -jet identification efficiency are determined using a new measurement technique which requires agreement between the measured cross sections with exactly one and with multiple identified b quarks from the top-quark decays. Assuming a top-quark mass of $175 \text{ GeV}/c^2$, a cross section of $8.5 \pm 0.6(\text{stat}) \pm 0.7(\text{syst})\text{pb}$ is measured.

DOI: 10.1103/PhysRevD.83.071102

PACS numbers: 14.65.Ha, 13.85.Ni, 13.85.Qk

I. INTRODUCTION

The properties of the top quark have been extensively studied since its discovery by the CDF and D0 collaborations at the Fermilab Tevatron in 1995 [1,2]. The top-antitop ($t\bar{t}$) production cross section has been measured in all detectable decay channels, and good agreement was found between the results and the perturbative QCD calculations [3]. At the Fermilab Tevatron, a $p\bar{p}$ collider with a center-of-mass energy of 1.96 TeV, the dominant standard model (SM) mechanisms for $t\bar{t}$ production are $q\bar{q}$ annihilation (85%) and gluon fusion (15%). For a top-quark mass of $175 \text{ GeV}/c^2$ the predicted total cross section is $\sigma_{t\bar{t}} = 6.7^{+0.6}_{-0.7} \text{ pb}$ [4]. Previous measurements have been limited by statistical uncertainties and by the uncertainty in the heavy-flavor jet identification efficiency at high energy [5].

The top-quark decays into a W boson and a b quark almost 100% of the time [3]. The signal significance is expected to be greatest in the lepton+jets channel, in which one W decays leptonically and the other W decays to quarks. These $t\bar{t}$ events contain a high-momentum charged lepton, four jets from the four final-state quarks, and an undetected neutrino. To enhance the $t\bar{t}$ purity, at least one jet in the event is usually required to be identified as originating from a bottom quark (b tagged) [5]. The b -tagging efficiency, needed as an input to the measurement, introduces one of the largest sources of systematic uncertainty [5]. In this paper we present a new technique to measure the $t\bar{t}$ cross section ($\sigma_{t\bar{t}}$) and determine the b -tagging efficiency in lepton+jets events, which reduces the systematic uncertainty of the measurement and allows a determination of the b -tagging efficiency directly in the $t\bar{t}$ sample. This is the first use of the $t\bar{t}$ sample for *in situ* calibration of the b -tagging efficiency. The improvements in the associated systematic uncertainties benefit directly

other analyses, particularly searches for the Higgs boson [6] and supersymmetric particles [7] or other scenarios of new physics [8].

II. SELECTION OF $t\bar{t}$ CANDIDATE EVENTS

Results reported here are obtained using 1.12 fb^{-1} of integrated luminosity collected between March 2002 and August 2006 by the Collider Detector at Fermilab (CDF II). CDF II [9] is a general-purpose particle detector located at one of the two interaction points of the Tevatron Collider. Charged-particle tracking is provided by an eight-layer silicon detector, surrounded by a 3.1 m long open-cell drift chamber, the central outer tracker (COT). Both are contained in a superconducting solenoid with a 1.4 T magnetic field. The silicon system provides three-dimensional hit information between radii of 1.4 cm and 28 cm, and allows one to measure the distance of closest approach of energetic tracks to the event vertex in the transverse plane (impact parameter, d_0) with a resolution of $\sim 40 \mu\text{m}$, including a $30 \mu\text{m}$ contribution from the beamspot. The excellent impact parameter resolution is critical to identify displaced tracks which are associated to bottom quarks resulting from top-quark decays. The COT covers the pseudorapidity [10] range $|\eta| < 1.1$ and provides a long lever arm for track curvature measurements. Outside the solenoid, electromagnetic and hadronic calorimeters arranged in projective towers surround the tracking volume and absorb photons, electrons, and hadrons with $|\eta| < 3.6$. Beyond the calorimeters, drift chambers track penetrating muons in the region $|\eta| < 1.0$.

The data were collected with two high- p_T lepton triggers, one of which requires a high- E_T electron ($E_T > 18 \text{ GeV}$) and the other a high- p_T muon ($p_T > 18 \text{ GeV}/c$). The trigger efficiency is $95.3 \pm 1.5\%$ ($89.1 \pm 1.6\%$) for

TABLE I. Summary of event yields and background expectations sorted by the number of jets in the event. Event totals before b tagging (Pretag) are listed in the first row; all other entries correspond to the sample with exactly one b -tagged jet, assuming the measured $t\bar{t}$ cross section of 8.5 pb. For events with more than two jets, the $H_T > 200$ GeV requirement is applied. Only statistical uncertainties are included.

	W + 1 jet	W + 2 jets	W + 3 jets	W + 4 jets	W + \geq 5 jets
Pretag	78 903	12 873	1515	507	132
Electroweak	43 ± 5	75 ± 10	18 ± 2	4.9 ± 0.6	1.1 ± 0.1
W + HF	594 ± 237	249 ± 100	47 ± 19	11 ± 4	1.7 ± 0.7
W + LF	862 ± 259	323 ± 97	49 ± 15	9 ± 3	1.7 ± 0.5
Non-W	44 ± 17	46 ± 19	17 ± 7	6 ± 2	1.5 ± 0.6
Background	1542 ± 352	693 ± 141	131 ± 25	31 ± 6	6 ± 1
$t\bar{t}$	11 ± 2	68 ± 12	132 ± 13	123 ± 12	40 ± 4
Total	1554 ± 352	761 ± 141	263 ± 28	154 ± 13	46 ± 4
Data events	1788	825	264	156	43

identified electrons (muons). Events are selected off-line by requiring the presence of an isolated [11] electron (muon) candidate with $E_T > 20$ GeV and $|\eta| < 1.1$ ($p_T > 20$ GeV/ c and $|\eta| < 1.0$), and at least three jets with $E_T > 20$ GeV and $|\eta| < 2$. Jets are clustered with a cone-based algorithm with a cone size $\Delta R \equiv \sqrt{\Delta\phi^2 + \Delta\eta^2} = 0.4$, and their energies are corrected for instrumental effects and excess energy from additional $p\bar{p}$ collisions [12]. The primary vertex position along the beam is required to lie within 60 cm of the nominal interaction point and to be consistent with the z position of the point of origin of the high- p_T lepton. Events with additional identified high- p_T leptons, or a track which forms a value compatible with the Z boson mass if combined with the primary lepton, are removed to suppress backgrounds. To account for the expected neutrino, we require large missing transverse energy [10], $E_T > 20$ GeV, which rejects $\sim 50\%$ of background events that do not contain a real W boson. Finally, as $t\bar{t}$ events typically have larger total transverse energy than background events, we require the H_T [10] to exceed 200 GeV. Table I includes the event count before b tagging (pretag) sorted by the number of jets in the event. In the one- and two-jet bins, where background dominates over the signal, the H_T requirement is not applied and the samples are used as control samples.

III. IDENTIFICATION OF b JETS

Requiring at least one jet to be b tagged considerably reduces the background. The b -tagging algorithm exploits the long lifetime of bottom hadrons by identifying decay vertices inside jets [5]. These vertices are reconstructed requiring a minimum of two or three tracks with an impact parameter significance (d_0/σ_{d_0}) greater than 3.0 or 2.0, respectively. Track combinations consistent with a K_S^0 or Λ are removed, and an upper limit of $d_0 = 0.15$ cm is used to reject interactions with detector material. We measure the two-dimensional displacement of the secondary vertex

from the primary interaction point projected along the jet axis (L_{2D}). A jet is b tagged if the vertex has L_{2D} significance ($L_{2D}/\sigma_{L_{2D}}$) larger than 6.0, where the uncertainty on L_{2D} includes contributions from both the primary and secondary vertex fits. The probability of misidentifying a light-flavor jet as a b -quark jet due to detector resolution (mistag rate) is $1.9 \pm 0.4\%$, estimated from secondary vertices reconstructed on the opposite side of the primary vertex with $L_{2D}/\sigma_{L_{2D}}$ significance less than -6.0 in a generic jet sample [13]. The mistag rate is corrected by a factor of 1.3 ± 0.1 to account for the remaining contribution of long-lived light-flavor hadrons (K_S and Λ) and material interactions that are present only at positive $L_{2D}/\sigma_{L_{2D}}$.

The $t\bar{t}$ acceptance calculation is based on the PYTHIA [14] Monte Carlo simulation, with the CTEQ5L parton distribution functions [15] and assuming a top mass of 175 GeV/ c^2 . Heavy-flavor decays are treated by EVTGEN [16]. Monte Carlo events are passed through a GEANT [17] simulation of the detector and subjected to the same selection requirements as the data. The total acceptance before b tagging is $4.3 \pm 0.1\%$ ($3.5 \pm 0.1\%$) for electron (muon) events and includes the branching fraction of the W boson, the geometric and kinematic acceptances, and the lepton identification and trigger efficiencies.

In previous cross section measurements [5], the tagging efficiency was needed as an input in order to perform the measurement. In those cases, the efficiency for the full $t\bar{t}$ event was determined from simulation, and a multiplicative scale factor (S_b) was applied to the efficiency found in the simulation to correct for the per-jet efficiency difference between data and simulation. This difference is caused by imperfections in the simulation, arising from, for example, incomplete description of the silicon detector, tracking efficiencies, and hadron decay modeling. The scale factor S_b was measured using high statistics data and simulation samples, enriched in heavy flavor by requesting nonisolated low- p_T leptons, and used to correct

the heavy-flavor tagging efficiency in all the simulated samples. In the current 1.12 fb^{-1} data sample, S_b has been measured to be $S_b = 0.95 \pm 0.05$, where the uncertainty is dominated by the extrapolation from the low- p_T calibration sample to typical $t\bar{t}$ jet energies [13]. Using this nominal scale factor in a $t\bar{t}$ sample, we expect $46 \pm 4\%$ of the events to have exactly one b -tagged jet and $22 \pm 3\%$ to have two or more b -tagged jets. Charm-quark jets which are b tagged are treated analogously to b -quark jets, but we assume a 10% uncertainty on the scale factor for charm, S_c .

IV. BACKGROUND ESTIMATION

The primary background process is direct W production with multiple jets, where the W boson decays leptonically. Smaller contributions come from QCD jet production in which the W signature is faked by jets appearing as electrons or by semileptonic b -hadron decays (non- W), and different electroweak processes: single-top-quark production, diboson (WW , WZ , and ZZ) production, and Z boson decays to tau pairs.

The W + jets contribution to the background is separated into events with and without heavy-flavor jets. To estimate the background contribution from W events with only light-flavor jets (N_{tag}^{W+LF}), the mistag rate is parametrized as a function of jet E_T , η , and number of tracks, as well as event total energy, number of primary vertices, and primary vertex z position. This parametrization is applied to the pretag data set, and the result is scaled down to the fraction of the data not attributed to a physics process with heavy flavor. The average mistag rate, for 50 GeV jets, is approximately 1.6%.

To determine the number of tags that originated from W events accompanied by heavy-flavor quarks, the fractions of W + jets events attributable to $Wb\bar{b}$, $Wc\bar{c}$, and Wc are estimated with ALPGEN Monte Carlo [18] with an interface to PYTHIA to model parton showering [19].

Since in the simulation heavy-flavor production may arise both from the soft-radiation evolution of a given event or directly from the parton configuration, a procedure to avoid double counting has been implemented [13]. The fractions of W + jets with heavy flavor (heavy-flavor fractions, F_i , where the index corresponds to the different contributions) are calibrated using data and simulated samples of inclusive jets. The bottom and charm fractions in the simulation are extracted from the generator information, while the equivalents in the data are obtained from template fits to the kinematic and dynamic properties of the tagged events. The measured heavy-flavor fraction calibration factor is consistent with unity, except in the one-jet bin, where the value for the data is about 30% higher, the difference is assigned as an uncertainty [13]. The expected number of W events with heavy-flavor (N_{tag}^{W+HF}) is estimated by multiplying these fractions by the number of pretag events (N_{pre}^W) and the tagging efficiency in these events (ϵ_i), measured from simulation and corrected by

the scale factor, $N_{\text{tag}}^{W+HF} = N_{\text{pre}}^W \sum_i \epsilon_i F_i$. The contribution of other backgrounds and the $t\bar{t}$ signal are removed from the N_{pre}^W pretag expectation: $N_{\text{pre}}^W = N_{\text{pre}}^{\text{data}} - N_{\text{pre}}^{\text{non-}W} - N_{\text{pre}}^{t\bar{t}} - N_{\text{pre}}^{\text{ewk}}$, where $N_{\text{pre}}^{\text{data}}$ is the number of pretag events, $N_{\text{pre}}^{t\bar{t}}$ is the number of pretag events attributed to $t\bar{t}$ production, $N_{\text{pre}}^{\text{non-}W}$ is the number of events without a W boson, and $N_{\text{pre}}^{\text{ewk}}$ is the contribution from single-top-quark production, Z boson decays to tau pairs, and diboson production. Both $N_{\text{pre}}^{\text{non-}W}$ and $N_{\text{pre}}^{\text{ewk}}$ are discussed below.

Some events without a W boson may satisfy the pretag requirements of an identified lepton and large missing energy. For example, photon conversions or misidentified pions or kaons may comply with the lepton requirements, and the missing energy may arise due to mismeasured jets. Heavy-flavor di-jet production may also result in leptons from the semileptonic decay faking the W boson signal. The expectation for this non- W background is determined from data, by fitting the missing energy distribution in each jet multiplicity bin. The templates used in the fit are derived from PYTHIA ($t\bar{t}$) and ALPGEN (W + jets) Monte Carlo, and samples enriched in fake leptons and heavy flavor. The sample with fake leptons is obtained from events in data where the primary lepton fails at least two identification requirements [20], while di-jet events with nonisolated low- E_T leptons provide the heavy-flavor enriched sample. The $t\bar{t}$ contribution is fixed to the value expected for the measured cross section. The fraction of non- W events is measured from the fits both before and after requiring a b -tagged jet.

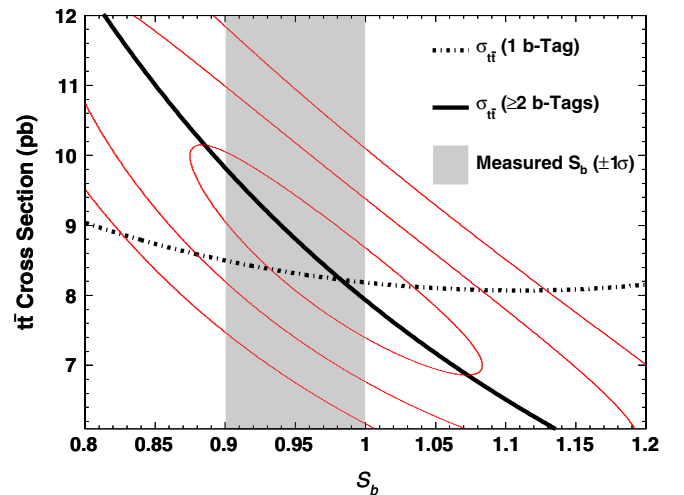


FIG. 1 (color online). Dependence of the exclusive single and multiple-tagged cross sections on the b -tagging efficiency scale factor. The point where the two measurements intersect is in good agreement with the independent determination of the b -tag scale factor from low- p_T data. The associated one, two, and three sigma confidence bands for the cross section and S_b are also shown.

TABLE II. Summary of event yields and background expectations sorted by the number of jets in the event, for events with at least two b -tagged jets, assuming the measured $t\bar{t}$ cross section of 8.5 pb. For events with more than two jets, the $H_T > 200$ GeV requirement is applied. Only statistical uncertainties are included.

	$W + 2$ jets	$W + 3$ jets	$W + 4$ jets	$W + \geq 5$ jets
Electroweak	7 ± 1	2.9 ± 0.4	0.9 ± 0.1	0.22 ± 0.03
$W + \text{HF}$	22 ± 9	6 ± 2	1.8 ± 0.7	0.3 ± 0.1
$W + \text{LF}$	3 ± 1	1.4 ± 0.4	0.4 ± 0.1	0.09 ± 0.03
Non- W	1.7 ± 0.7	1.4 ± 0.5	0.5 ± 0.2	0.12 ± 0.05
Background	35 ± 9	12 ± 3	3.5 ± 0.8	0.7 ± 0.1
$t\bar{t}$	20 ± 4	54 ± 10	69 ± 12	25 ± 4
Total	55 ± 10	66 ± 10	73 ± 12	26 ± 4
Data events	63	64	72	29

A Monte Carlo-based method is used to estimate the remaining backgrounds due to single top quark production (PYTHIA/MADEVENT [21]), vector boson pair production (PYTHIA) and $Z \rightarrow \tau\tau$ (ALPGEN interfaced to PYTHIA), normalizing the expectations to their respective theoretical cross sections [22]. The tagging efficiency is taken from these Monte Carlo samples and corrected by S_b .

V. RESULTS

The scale factor is applied to the tagging efficiency in the signal term as well as in the $W +$ jets with heavy flavor and electroweak backgrounds. Instead of using the S_b value measured in the low- p_T lepton sample, in this paper we perform a simultaneous fit of the $t\bar{t}$ cross section and S_b by requiring that the single and multiple-tagged samples correspond to the same $t\bar{t}$ cross section. Since the $W +$ jets backgrounds and, to a lesser extent, the non- W background

depend on the assumed $t\bar{t}$ cross section, the procedure to determine them is iterative. The $t\bar{t}$ contribution to the b -tagged sample is written as $N_{\text{tag}}^{t\bar{t}} = N_{\text{tag}} - N_{\text{tag}}^{W+\text{HF}} - N_{\text{tag}}^{W+\text{LF}} - N_{\text{tag}}^{\text{ewk}} - N_{\text{tag}}^{\text{non-}W}$. Figure 1 shows the cross section measurement for exclusive single b -tagged events, and for events with two or more b -tagged jets as a function of S_b . A Poisson likelihood fit yields results of $\sigma_{t\bar{t}} = 8.2 \pm 0.9$ pb with only the statistical and scale factor uncertainties included, and $S_b = 0.98 \pm 0.07$, consistent with the S_b value measured in the low- p_T lepton sample. The associated confidence bands are also shown in Fig. 1. The signal and background contributions to the b -tagged data sample are summarized in Tables I and II for the single and the multiple-tagged data, respectively, and are shown in Fig. 2 as a function of the jet multiplicity.

The systematic uncertainties on the cross section, before b -tagging requirements, are dominated by a 4.2% uncertainty due to the jet energy calibration. Other sources of uncertainty are the choice of Monte Carlo generator (2.1%), the lepton identification efficiency (2.0%), the choice of parton distribution functions (0.7%), and the modeling of initial and final-state radiation (0.5%). The uncertainty in the integrated luminosity is 6% [23]. A 3.3% uncertainty associated to the background estimation was determined using a large ensemble of simulated experiments by fluctuating the backgrounds within their uncertainties. The different sources of systematic uncertainty are added in quadrature for the signal expectation [5].

In order to include the independent measurement of the S_b in the lepton sample ($S_b = 0.95 \pm 0.05$), a term to penalize deviations from this value is added to the likelihood. With this constraint we measure a cross section of $8.5 \pm 0.6(\text{stat}) \pm 0.7(\text{syst})\text{pb}$ and a scale factor of 0.96 ± 0.04 . With this S_b the fraction of selected $t\bar{t}$ candidates

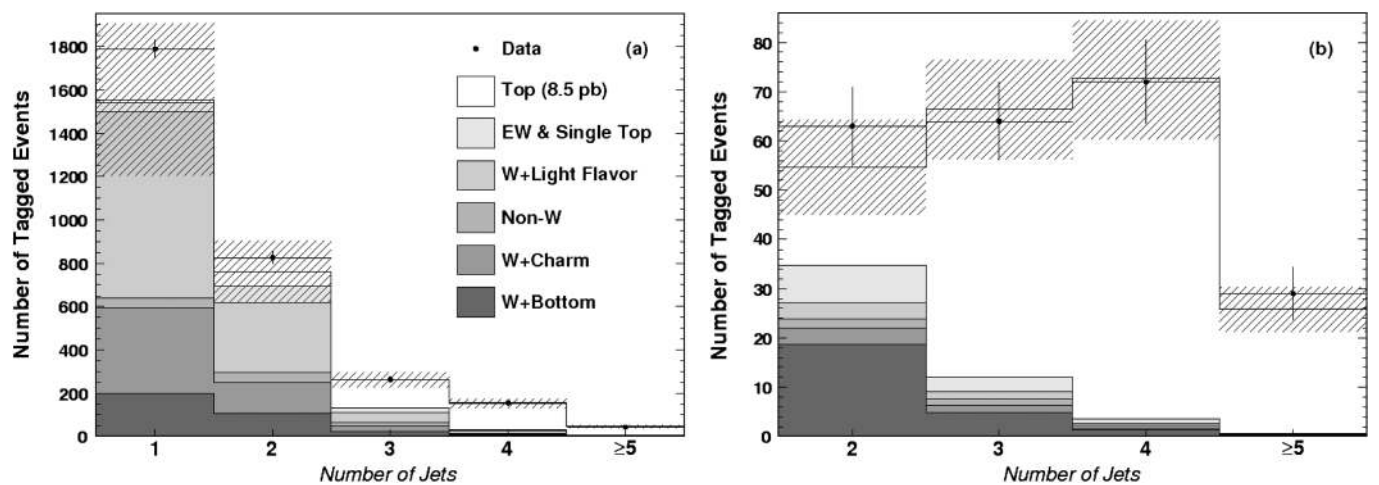


FIG. 2. Summary of background and signal event yields versus number of jets in the event when requiring (a) one b -tagged jet and (b) at least two b -tagged jets. The $t\bar{t}$ contribution is normalized to the measured cross section. The H_T requirement is released for events with fewer than three jets. The hashed region shows the total systematic uncertainty on the expectation.

with exactly one identified b quark is $46 \pm 4\%$ and with two or more b quarks is $23 \pm 3\%$. The statistical uncertainty of $\sigma_{t\bar{t}}$ also includes the uncertainty on S_b .

In conclusion, we have performed the first simultaneous fit of the $t\bar{t}$ production cross section and the b -tagging efficiency in $p\bar{p}$ collisions at $\sqrt{s} = 1.96$ TeV using data corresponding to an integrated luminosity of 1.12 fb^{-1} . The cross section result, $8.5 \pm 0.6(\text{stat}) \pm 0.7(\text{syst})\text{pb}$, is consistent with the SM expectation of $6.7_{-0.7}^{+0.6}$ pb for a mass of $175 \text{ GeV}/c^2$. The dependence of the acceptance on the top mass results in a variation of the measured cross section by ± 0.1 pb for every $\mp 1 \text{ GeV}/c^2$ shift in the assumed top-quark mass. With the innovative technique presented in this paper, the b -tagging efficiency for high- E_T b jets was directly measured in the $t\bar{t}$ sample, and its uncertainty reduced with respect to previous results [5]. Future measurements at the Large Hadron Collider, like searches for the Higgs boson and supersymmetric particles, where b -tagging performance is critical, could benefit from this technique.

ACKNOWLEDGMENTS

We thank the Fermilab staff and the technical staffs of the participating institutions for their vital contributions. This work was supported by the U.S. Department of Energy and National Science Foundation; the Italian Istituto Nazionale di Fisica Nucleare; the Ministry of Education, Culture, Sports, Science and Technology of Japan; the Natural Sciences and Engineering Research Council of Canada; the National Science Council of the Republic of China; the Swiss National Science Foundation; the A.P. Sloan Foundation; the Bundesministerium für Bildung und Forschung, Germany; the World Class University Program, the National Research Foundation of Korea; the Science and Technology Facilities Council and the Royal Society, UK; the Institut National de Physique Nucleaire et Physique des Particules/CNRS; the Russian Foundation for Basic Research; the Ministerio de Ciencia e Innovación, and Programa Consolider-Ingenio 2010, Spain; the Slovak R&D Agency; and the Academy of Finland.

-
- [1] F. Abe *et al.*, (CDF Collaboration), *Phys. Rev. Lett.* **74**, 2626 (1995).
- [2] S. Abachi *et al.* (D0 Collaboration), *Phys. Rev. Lett.* **74**, 2632 (1995).
- [3] C. Amsler *et al.*, (Particle Data Group), *Phys. Lett. B* **667**, 1 (2008).
- [4] M. Cacciari *et al.*, *J. High Energy Phys.* 09 (2008) 127; N. Kidonakis and R. Vogt, *Phys. Rev. D* **78**, 074005 (2008); S. Moch and P. Uwer, *Phys. Rev. D* **78**, 034003 (2008).
- [5] A. Abulencia *et al.*, (CDF Collaboration), *Phys. Rev. Lett.* **97**, 082004 (2006); D. Acosta *et al.* (CDF Collaboration), *Phys. Rev. D* **71**, 052003 (2005).
- [6] T. Aaltonen *et al.* (CDF Collaboration), *Phys. Rev. Lett.* **103**, 101802 (2009).
- [7] T. Aaltonen *et al.* (CDF Collaboration), *Phys. Rev. D* **82**, 092001 (2010).
- [8] T. Affolder *et al.* (CDF Collaboration), *Phys. Rev. Lett.* **84**, 835 (2000).
- [9] F. Abe *et al.* (CDF Collaboration), *Nucl. Instrum. Methods Phys. Res., Sect. A* **271**, 387 (1988); D. Acosta *et al.* (CDF Collaboration), *Phys. Rev. D* **71**, 032001 (2005); A. Abulencia *et al.* (CDF Collaboration), *J. Phys. G* **34**, 2457 (2007).
- [10] A cylindrical coordinate system with the z axis along the proton direction is used, in which θ is the polar angle. We define $E_T = E \sin\theta$, $p_T = p \sin\theta$, and pseudorapidity $\eta = -\text{Intan}(\theta/2)$. The missing transverse energy is defined by $E_T = -\sum_i E_T^i \hat{n}_i$, where i is the calorimeter tower number and \hat{n}_i is a unit vector perpendicular to the beam axis and pointing at the i th calorimeter tower. The missing transverse energy is corrected for jets and muons. The H_T is defined by the scalar sum of the E_T , the lepton transverse momentum, and the total jet transverse energy.
- [11] The energy inside a cone of radius $R = \sqrt{(\Delta\phi)^2 + (\Delta\eta)^2} = 0.4$ around the lepton is required to be less than 10% of the electron (or muon) E_T (p_T).
- [12] A. Bhatti *et al.*, *Nucl. Instrum. Methods Phys. Res., Sect. A* **566**, 375 (2006).
- [13] D. Sherman, Ph.D. thesis, Harvard University [Fermilab-Thesis-2007-82, 2007].
- [14] T. Sjöstrand *et al.*, *Comput. Phys. Commun.* **135**, 238 (2001).
- [15] J. Pumplin *et al.*, *J. High Energy Phys.* 07 (2002) 012.
- [16] D.J. Lange, *Nucl. Instrum. Methods Phys. Res., Sect. A* **462**, 152 (2001).
- [17] R. Brun and F. Carminati, CERN, Programming Library Long Writeup No. W 5013, 1993.
- [18] M.L. Mangano *et al.*, *J. High Energy Phys.* 07 (2003) 001.
- [19] T. Sjostrand *et al.*, *Comput. Phys. Commun.* **135**, 238 (2001).
- [20] T. Aaltonen *et al.* (CDF Collaboration), *Phys. Rev. D* **80**, 052001 (2009).
- [21] J. Alwall *et al.*, *J. High Energy Phys.* 09 (2007) 028.
- [22] J. Campbell and R.K. Ellis, *Phys. Rev. D* **60**, 113006 (1999); B. Harris *et al.*, *Phys. Rev. D* **66**, 054024 (2002).
- [23] D. Acosta *et al.*, *Nucl. Instrum. Methods Phys. Res., Sect. A* **494**, 57 (2002); S. Klimenko, J. Konigsberg, and T.M. Liss, Report No. FERMILAB-FN-0741, 2003.